

**<sup>54</sup>Fe HETEROGENEITY IN SEQUENTIAL ACID LEACHATES OF REFRACTORY INCLUSIONS.**

Q.R. Shollenberger<sup>1</sup>, H. Tang<sup>1</sup>, and E. D. Young<sup>1</sup>, <sup>1</sup>Department of Earth, Planetary, and Space Sciences, University of California Los Angeles, Los Angeles, CA, USA (qshollenberger@ucla.edu)

**Introduction:** Calcium-aluminum-rich inclusions (CAIs) are the first solids to condense in the protoplanetary disk and their isotopic compositions provide information about the formation and evolution of the early Solar System. Previous work has shown for a variety of elements that isotopic differences exist between normal (non-FUN) CAIs and later formed Solar System solids [e.g., 1-2]. For Ca and Ti, and the Fe-peak elements, including Cr and Ni in CAIs, previous studies have attributed the isotopic differences to mass dependent isotope fractionation processes such as condensation and evaporation, nucleosynthetic variations, or both [e.g., 3-7]. Importantly, these studies report that CAIs typically have the largest nucleosynthetic anomaly in the most neutron-rich isotope of these elements (*i.e.*, <sup>48</sup>Ca, <sup>50</sup>Ti, <sup>54</sup>Cr, <sup>64</sup>Ni). However, only two studies have reported Fe nucleosynthetic variability in normal CAIs [8-9], and it is currently unclear which Fe isotope(s) is anomalous.

To address this issue, we present the Fe isotopic compositions of three bulk CAIs along with six sequential acid leachates obtained on each CAI. Previous studies have shown that chemical separation of meteoritic components via acid leaching are able to concentrate different meteorite phases in the various leaching steps, thus providing important information regarding the carrier phases of the isotopically anomalous material [e.g., 10]. Similarly, the goal of our leaching procedure is to chemically separate the different Fe-bearing phases present in our CAI samples in order to distinguish pristine Fe that condensed into the CAI upon formation versus Fe that was added to the CAI at a later time (*e.g.*, secondary alteration). We use this dataset to better understand the isotopic material present in the early Solar System and the condensation history of CAIs.

**Samples and Methods:** Three different types of CAIs (Table 1) were obtained. A small fraction of each CAI powder was reserved for the bulk CAI Fe isotope measurement while the majority of each CAI powder was processed through the following sequential acid leaching procedure modified from [10].

- 1) 0.9mL acetic acid + 0.9mL H<sub>2</sub>O, 1 day, 20 °C
- 2) 0.6mL HNO<sub>3</sub> + 1.2mL H<sub>2</sub>O, 5 days, 20 °C
- 3) 0.83mL HCl + 0.97mL H<sub>2</sub>O, 1 day, 75 °C
- 4) 0.9mL HF + 0.45mL HCl + 0.45mL H<sub>2</sub>O, 1 day, 75 °C
- 5) 0.9mL HF + 0.9mL HCl, 3 days, 150 °C
- 6) 0.6mL HNO<sub>3</sub> + 1.2mL HF + 34μL HClO<sub>4</sub>, 5 days, 180 °C

The CAI powders for the bulk measurements were digested on hot plates using 5 mL of a 3:1 concentrated HF-HNO<sub>3</sub> mixture followed by 3 mL of reverse aqua regia to achieve complete dissolution. Chemical separation of Fe from the bulk CAIs and leachate samples followed previously established procedures [11-12].

**Table 1** – Characteristics of the CAIs in this study.

CAI	Host meteorite	Mass for leaching (mg)	Mass for bulk Fe measurement (mg)	Description
Warrior	Acfer 082 (CV3)	92.5	15.8	FTA – FG
Pigeon	Acfer 082 (CV3)	50.3	4.6	CTA – FMG
Lizard	Allende (CV3.6)	22.8	8.2	A – FG

FTA = fluffy Type A, CTA = compact Type A, A = Type A, FG = fine-grained, FMG = fine- to medium-grained

The Fe isotope compositions of the samples and standards were collected in medium resolution mode utilizing multicollector inductively coupled plasma mass spectrometry (MC-ICPMS, ThermoFinnigan Neptune™) at UCLA. Instrumental mass bias was corrected using the sample-standard bracketing technique with the IRMM-014 reference material to obtain mass dependent compositions. To obtain Fe mass independent (nucleosynthetic) data, instrumental and natural mass fractionation were corrected using the exponential law and normalizing to <sup>57</sup>Fe/<sup>56</sup>Fe = 0.023095.

**Results and Discussion:** Shown in Fig. 1 are the mass dependent Fe isotope compositions of our samples expressed utilizing the δ-notation (parts per thousand deviation from IRMM-014). Our range in δ<sup>56/54</sup>Fe values is consistent with previous values for bulk CAIs [9,13]. Most of our samples plot along a trendline (black) with a slope of 0.671±0.006, consistent with the slope for kinetic isotope fractionation of 0.672 (curvature of the fractionation line in δ-δ space is small over this range), demonstrating that our samples have experienced various condensation and evaporation events. However, Pigeon leachate steps 3-6 deviate from the kinetic isotope fractionation line. In an Fe three isotope diagram, a trend with a slope of 1 would indicate that there is a nucleosynthetic anomaly for <sup>54</sup>Fe. Given that our four Pigeon leachates define their own trend (green) with a slope of 0.88±0.02, we conclude that there is a nucleosynthetic anomaly mainly on <sup>54</sup>Fe and not <sup>56</sup>Fe or <sup>57</sup>Fe. This observation is further supported by the fact that when the data are normalized to <sup>57</sup>Fe/<sup>54</sup>Fe, an apparent anomaly is present on <sup>58</sup>Fe which is otherwise absent when the data are normalized using <sup>57</sup>Fe/<sup>56</sup>Fe.

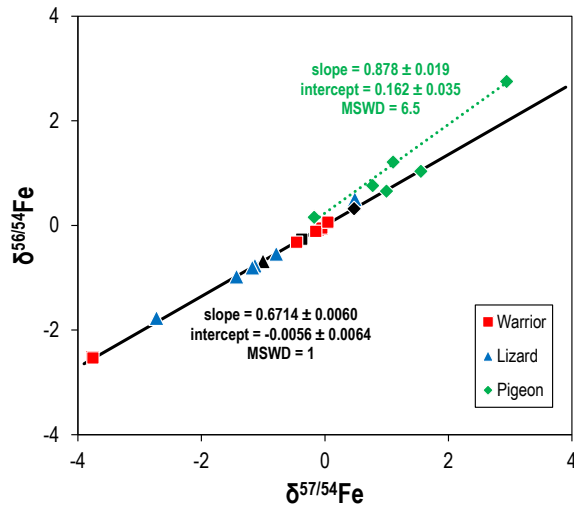


Fig. 1 – Three isotope diagram for  $\delta^{56/54}\text{Fe}$  versus  $\delta^{57/54}\text{Fe}$  for our bulk CAIs (black symbols) and their corresponding leachates.

Shown in Fig. 2 are the mass-independent  $^{54}\text{Fe}$  isotope compositions expressed using the  $\epsilon$ -notation (parts per ten thousand deviation from IRMM-014). We do not observe any resolved anomalies on  $^{58}\text{Fe}$ . Our bulk CAIs have small excesses in  $\epsilon^{54}\text{Fe}$  (Fig. 2a), with the exception of Pigeon, and are in agreement with the average bulk CAI value from [9]. Most of the early leaching steps have small excesses in  $^{54}\text{Fe}$  (Fig. 2a) and are similar to the bulk CAI values within the analytical uncertainties. The  $\epsilon^{54}\text{Fe}$  compositions from Fig. 2a are similar to the  $^{54}\text{Fe}$  anomalies reported for bulk chondrites from [14]. In comparison, the later leaching steps have much larger and variable deficits in  $^{54}\text{Fe}$  (Fig. 2b), consistent with previously reported data on the CAI Egg 2 [9].

Overall, the leaching procedure is effective in separating the various Fe-bearing phases of our CAIs. For example, most of our early leaching steps have  $^{54}\text{Fe}$  anomalies that are similar to bulk CAIs and bulk chondrites (Fig. 2a). In comparison, the later leaching steps demonstrate that a phase is present in CAIs with deficits in  $^{54}\text{Fe}$ , most clearly demonstrated by the Pigeon leachates. We investigated three different kinds of Type A inclusions, and all of our samples provide evidence for an Fe-bearing phase characterized by deficits in  $^{54}\text{Fe}$  that is chemically resistant.

Compared to refractory elements like Ti and Ca, Fe is not predicted to be a major constituent of CAIs due to its lower condensation temperature. Importantly, CAIs have nucleosynthetic Ca and Ti anomalies that are distinct from bulk meteorites [e.g., 3-5]. However, this work shows that bulk CAIs have Fe isotope anomalies that are indistinguishable at the current level of precision from bulk meteorites. This likely indicates

that most of the Fe in the CAI forming region/process was present in the gas phase, as expected based on its volatility, and had a  $^{54}\text{Fe}$  composition similar to bulk meteorites because Fe is well mixed in the gas phase. However, the  $^{54}\text{Fe}$  deficits in our later leachate samples likely derive from refractory dust incorporated into CAIs. The isotopically distinct Fe from the dust is such a small fraction of the total CAI Fe budget that it is only revealed with an acid leaching procedure that essentially removes all the CAI Fe derived from the gas phase. The mineralogical host for the refractory Fe component is to be determined.

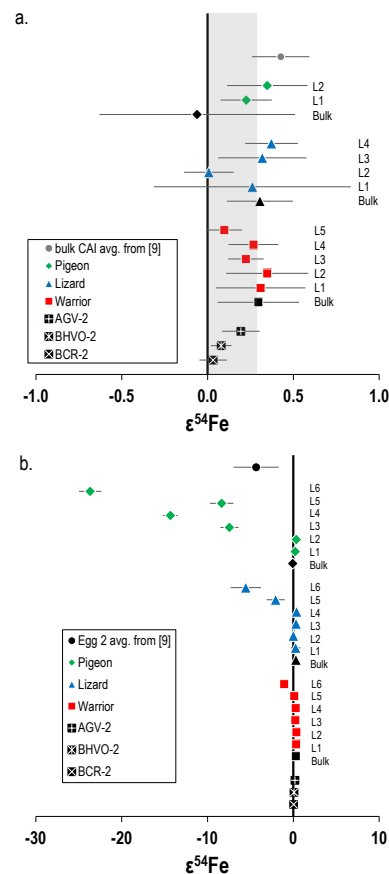


Fig. 2a/b – The  $\epsilon^{54}\text{Fe}$  data for the three CAIs and their leachates as well as geological standards. Leachates are labeled for each CAI. Grey box in a) represents the range of bulk chondrites from [14]. Note the different scales.

**Acknowledgments:** This work was funded by a Deutsche Forschungsgemeinschaft (DFG, German Research Foundation) research fellowship (project number 440227108).

**References:** [1] Dauphas & Schauble (2016) *Annu. Rev. Earth Planet. Sci.*, **44**, 709. [2] Burkhardt et al. (2019) *GCA*, **261**, 145. [3] Huang et al. (2012) *GCA*, **77**, 252. [4] Simon et al. (2017) *EPSL*, **472**, 277. [5] Davis et al. (2018) *GCA*, **221**, 275. [6] Render et al. (2018) *ApJ*, **862**, 26. [7] Mercer et al. (2015) *LPSC*, **46**, #2920. [8] Völkering & Papanastassiou (1989) *ApJ*, **347**, L43. [9] Shollenberger et al. (2019) *GCA*, **263**, 215. [10] Reisberg et al. (2009) *EPSL*, **277**, 334. [11] Dauphas et al. (2009) *Chem. Geol.*, **267**, 175. [12] Jordan et al. (2019) *GCA*, **246**, 461. [13] Mullane et al. (2005) *EPSL*, **239**, 203. [14] Schiller et al. (2020) *Sci. Adv.*, **6**, eaay7604.